Observing the nonvectorial yet cotranslational folding of a multidomain protein, LDL receptor, in the ER of mammalian cells.

著者	Hiroshi Kadokura, Yui Dazai, Yo Fukuda, Naoya Hirai, Orie Nakamura, Kenji Inaba
journal or publication title	Proceedings of the National Academy of Sciences of the United States of America
volume	117
number	28
page range	16401-16408
year	2020-07-14
URL	http://hdl.handle.net/10097/00130870

doi: 10.1073/pnas.2004606117

Observing the nonvectorial yet cotranslational folding of a multidomain protein, LDL receptor, in the ER of mammalian cells

Hiroshi Kadokura[a,1], Yui Dazai[a], Yo Fukuda[a], Naoya Hirai[a], Orie Nakamura[a], and Kenji Inaba[a]

[a]Institute of Multidisciplinary Research for Advanced Materials, Tohoku University, Miyagi 980-8577, Japan

Edited by Jonathan S. Weissman, University of California, San Francisco, CA, and approved May 31, 2020 (received for review March 10, 2020)

Proteins have evolved by incorporating several structural units within a single polypeptide. As a result, multidomain proteins constitute a large fraction of all proteomes. Their domains often fold to their native structures individually and vectorially as each domain emerges from the ribosome or the protein translocation channel, leading to the decreased risk of interdomain misfolding. However, some multidomain proteins fold in the endoplasmic reticulum (ER) nonvectorially via intermediates with nonnative disulfide bonds, which were believed to be shuffled to native ones slowly after synthesis. Yet, the mechanism by which they fold nonvectorially remains unclear. Using two-dimensional (2D) gel electrophoresis and a conformation-specific antibody that recognizes a correctly folded domain, we show here that shuffling of nonnative disulfide bonds to native ones in the most N-terminal region of LDL receptor (LDLR) started at a specific timing during synthesis. Deletion analysis identified a region on LDLR that assisted with disulfide shuffling in the upstream domain, thereby promoting its cotranslational folding. Thus, a plasma membrane-bound multidomain protein has evolved a sequence that promotes the nonvectorial folding of its upstream domains. These findings demonstrate that nonvectorial folding of a multidomain protein in the ER of mammalian cells is more coordinated and elaborated than previously thought. Thus, our findings alter our current view of how a multidomain protein folds nonvectorially in the ER of living cells.

LDL receptor | cotranslational folding | multidomain protein | nonvectorial folding | disulfide bonds

Incorporating several structural domains into a single polypeptide is a strategy for generating proteins with novel functions in both prokaryote and eukaryote. In eukaryote, more than two-thirds of all proteins contain multiple domains (1). Their domains often fold individually and vectorially one after another as they emerge from the ribosome (2–6). Multidomain proteins tend to be highly vulnerable to misfolding and aggregation, probably due to undesired interactions between domains (7–10). It is generally believed that vectorial folding is preferable for multidomain proteins as temporal and spatial separation of individual domains limit the total number of available conformations, leading to the decreased risk of misfolding (2, 3, 11).

In mammalian cells, approximately one-thirds of the proteins in the genome will enter the endoplasmic reticulum (ER) for their folding in this compartment. The folding and activity of most of these proteins require the formation of proper disulfide bonds in them (12–15), and failure in the process can lead to serious disease conditions (14). Thus, understanding the mechanisms of disulfide bond formation in these proteins is important. The ER of mammalian cells harbors ∼20 protein disulfide isomerase (PDI) family members that are thought to introduce disulfide bonds into nascent polypeptide chains (12–14, 16). However, when and how disulfide bonds form in the chains remains poorly understood.

A large number of secretory and membrane-bound proteins in human cells contain not only disulfide bonds but also multiple domains (13). To decrease the risk of misfolding, their domains often fold vectorially as their domains appear from the protein translocation channel (11, 17, 18). However, increasingly, proteins have been identified that likely fold nonvectorially in the ER via intermediates with nonnative disulfides (19–23) (*SI Appendix*, Fig. S1). Yet, how and why their folding proceeds nonvectorially in the ER remained largely unclear.

Low-density lipoprotein receptor (LDLR) is an intensively studied plasma membrane-bound multidomain protein containing three disulfide bonds in each of its seven cysteine-rich domains (R1–R7) and three epidermal growth factor-like domains (EGF1–EGF3) (Fig. 1*A*) (24–26). This protein plays a central role in mammalian cholesterol metabolism by transporting cholesterol-containing lipoprotein particles from the circulation into cells. Impaired folding of LDLR can result in hypercholesterolemia and increased risk of coronary heart disease, underlining the importance of understanding its folding mechanisms (24–26). Evidence indicates that nonnative disulfides formed at the early stage of folding are shuffled (isomerized) to native disulfide bonds (19, 20, 27, 28) through the catalysis of a PDI family member(s) (12, 27). The shuffling reaction had been thought to be rate-limiting in the folding pathway (*SI Appendix*, Fig. S1), occurring over tens of minutes after synthesis (19, 20). A similar two-step mechanism is likely adopted by a number of

Significance

Multidomain proteins constitute more than two-thirds of all proteome. To decrease the risk of misfolding, these proteins generally fold vectorially as each domain emerges from the ribosome or protein translocation channel. Interestingly, however, some cell surface multidomain proteins including the low-density lipoprotein receptor (LDLR) fold in the ER nonvectorially via intermediates with nonnative disulfides. Shuffling of nonnative disulfides to native ones, a key step in their folding, has been thought to proceed slowly after synthesis. Here, we find that disulfide shuffling in LDLR occurs at a specific timing during synthesis in a manner depending on a downstream region of the polypeptide. Thus, nonvectorial folding of multidomain proteins in the endoplasmic reticulum (ER) may be more coordinated and elaborated than thought.

Author contributions: H.K., Y.D., and Y.F. designed research; H.K., Y.D., Y.F., N.H., and O.N. performed research; H.K., Y.D., Y.F., N.H., O.N., and K.I. analyzed data; and H.K. and K.I. wrote the paper.

The authors declare no competing interest.

This article is a PNAS Direct Submission.

[1]To whom correspondence may be addressed. Email: hiroshi.kadokura.b3@tohoku.ac.jp.

This article contains supporting information online at https://www.pnas.org/lookup/suppl/doi:10.1073/pnas.2004606117/-/DCSupplemental.

First published June 29, 2020.

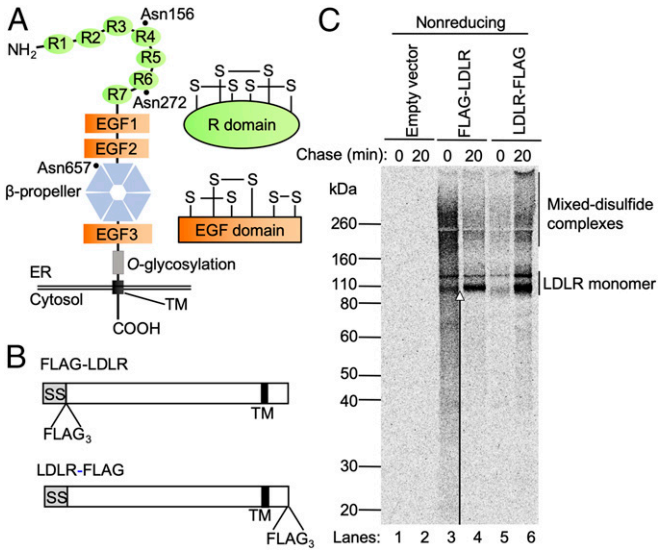

Fig. 1. Elongating chains of LDLR purified from cells. (*A*) Domain organizations of the LDLR. LDLR contains N-terminally located seven cysteine-rich domains (R1–R7), each stabilized by three disulfide bonds (*Upper Right*). Two EGF domains (EGF1 and EGF2) are followed by a six-bladed β-propeller domain and a third EGF domain (EGF3). Each EGF domain contains three disulfide bonds (*Lower Right*). The regions other than the R and EGF domains do not contain disulfide bonds. Dots, N-glycosylation sites (34); *O*-glycosylation, *O*-glycosylation region; TM, transmembrane domain (19). (*B*) Structures of FLAG-tagged LDLR constructs. SS, signal sequence. (*C*) HeLa cells expressing the indicated LDLR variants were pulse-labeled for 2 min, chased for 0 or 20 min, alkylated with NEM, immunoprecipitated with anti-FLAG antibody, and analyzed by nonreducing SDS/PAGE. Open arrow, the elongating chains of LDLR.

proteins (21) including those that obligately require reducing power for folding (22, 23). However, since these preceding works studied the behavior of the full-length products, when and how each step in the folding actually takes place after initiation of their synthesis remained unclear. Here, we studied the cotranslational folding of LDLR in the ER of living mammalian cells. We found that disulfide shuffling in an R domain started at a specific timing during the synthesis of the protein and that a region downstream of the R domain was responsible for the disulfide shuffling that occurred cotranslationally. Thus, in contrast to the previous view that nonvectorial folding of multidomain proteins in the ER is a slow process that occurs posttranslationally (13), it can be highly coordinated and elaborated in living mammalian cells.

Results

Observing Disulfide Bond Formation in the Elongating Chains of LDLR. To investigate the cotranslational folding of LDLR, we inserted a triple-FLAG tag either at the N terminus of LDLR after the signal sequence cleavage site (FLAG-LDLR) or after the C terminus of the protein (LDLR-FLAG) (Fig. 1*B*) as we have done before with bacterial alkaline phosphatase (29). Anti-FLAG antibody can pull down elongating polypeptides from the former but not the latter construct (29, 30). HeLa cells expressing these constructs were pulse-labeled for 2 min with [^{35}S]-methionine and [^{35}S]-cysteine and chased for 20 min in the absence of radioactivity. To freeze the oxidation status of proteins, we treated cells directly with strong acid and alkylated free cysteines with *N*-ethylmaleimide (NEM) (31). The NEM-alkylated cellular proteins were immunoprecipitated with anti-FLAG antibody and analyzed by sodium dodecyl sulfate–polyacrylamide gel electrophoresis (SDS/PAGE) (Fig. 1*C*). For the N-terminally tagged construct, we observed smeared bands ending at the positions of LDLR full-length monomer (indicated by an upward arrow on lane 3). They represent elongating chains of LDLR for the following reasons. First, they were observed when the elongating chains of LDLR were purified from the N-terminally tagged construct (lane 3), but not when the full-length LDLR was purified from the C-terminally tagged construct (lane 5). Second, after 20 min of chase, the intensities of these smeared bands became fainter, with a concomitant increase in the amount of LDLR full-length monomer (lane 4).

To analyze disulfide bond formation in the elongating chains, samples were separated by two-dimensional (2D) SDS/PAGE in which the first dimension was nonreducing and the second reducing (Fig. 2*A*). On the gels, the distinct electrophoretic mobilities of proteins containing disulfide bonds before and after reduction cause deviations from the diagonal, allowing analysis of oxidation status of elongating chains as a function of chain length: Chains with intramolecular disulfides run on the right of the diagonal, those with intermolecular disulfides run on the left (29, 32). Notably, actual detection of the signals corresponding to the elongating chains of LDLR on 2D gels usually required the exposure of the imaging plate to the gels of the radiolabeled proteins for a month or more possibly because of the smallness of the number of growing chains of a certain chain length (33). The elongating chains of LDLR were observed as two distinct populations (Fig. 2*A*). One population appeared as a continuous signal along the diagonal, beginning at the smallest detectable size (<20 kDa) and ending at the size of full-length LDLR (~140 kDa). The second population of elongating chains appeared as a distinct and reproducible pattern of streaks to the right of the diagonal, beginning at the size of 30 kDa and also ending at the size of full-length LDLR as measured in the reducing dimension. Because the polypeptides on the latter streaks ran faster under nonreducing conditions than their reduced forms, they represent intramolecularly oxidized chains.

Timing of N-Glycosylation and Disulfide Bond Formation in the Elongating Chains of LDLR. The distribution of radioactivity within the trace of the oxidized chains of LDLR was uneven (Fig. 2*A*). While the regions of high radioactivity generally indicate pause sites in the synthesis of chains, the regions of low radioactivity correspond to the addition of *N*-glycan or a sequence that is translated at a higher rate than the surrounding codons (18). LDLR is a type I membrane protein containing three Asn residues that are known to receive *N*-glycan (Asn156, Asn272, and Asn657) (34). To study the timing of N-glycosylation at each residue, we introduced a substitution mutation into them. The regions of low radioactivity observed at the sizes of ~35 kDa and ~60 kDa in the WT LDLR (Fig. 2*A*) were absent in the LDLR N156Q and N272Q mutants, respectively (Fig. 2 *B* and *C*). They are therefore likely caused by core glycan addition to Asp156 and Asp272, respectively.

As we have seen above, disulfide bonds started to form on the polypeptides when they were elongated to 30 kDa. Importantly, the polypeptides were already oxidized when they received *N*-glycan at Asn156 (Fig. 2 *A–D*). We used this fact to estimate the length of polypeptide chains in amino acids at the initiation of disulfide bond formation as follows. Polypeptide chains entering the ER lumen are often cotranslationally modified with *N*-glycan by the oligosaccharyl–transferase complex (OST), an integral component of the protein translocation machinery (35). The distance between the ribosome P site and the OST active site is ~70 amino acids (11). Therefore, a nascent chain must have a minimum of ~70 amino acids after the glycosylation sequence for it to receive the *N*-glycan. Thus, the carboxyl-terminal residues of the elongating chains at the timing of N-glycosylation of Asn156 and Asn272 are estimated to be Ser226 and Asp342, respectively (Fig. 2 *E* and *F*). As we have described above, when the polypeptides received the first *N*-glycan, they were already oxidized (Fig. 2 *A–D*). Thus, disulfide bonds likely started to

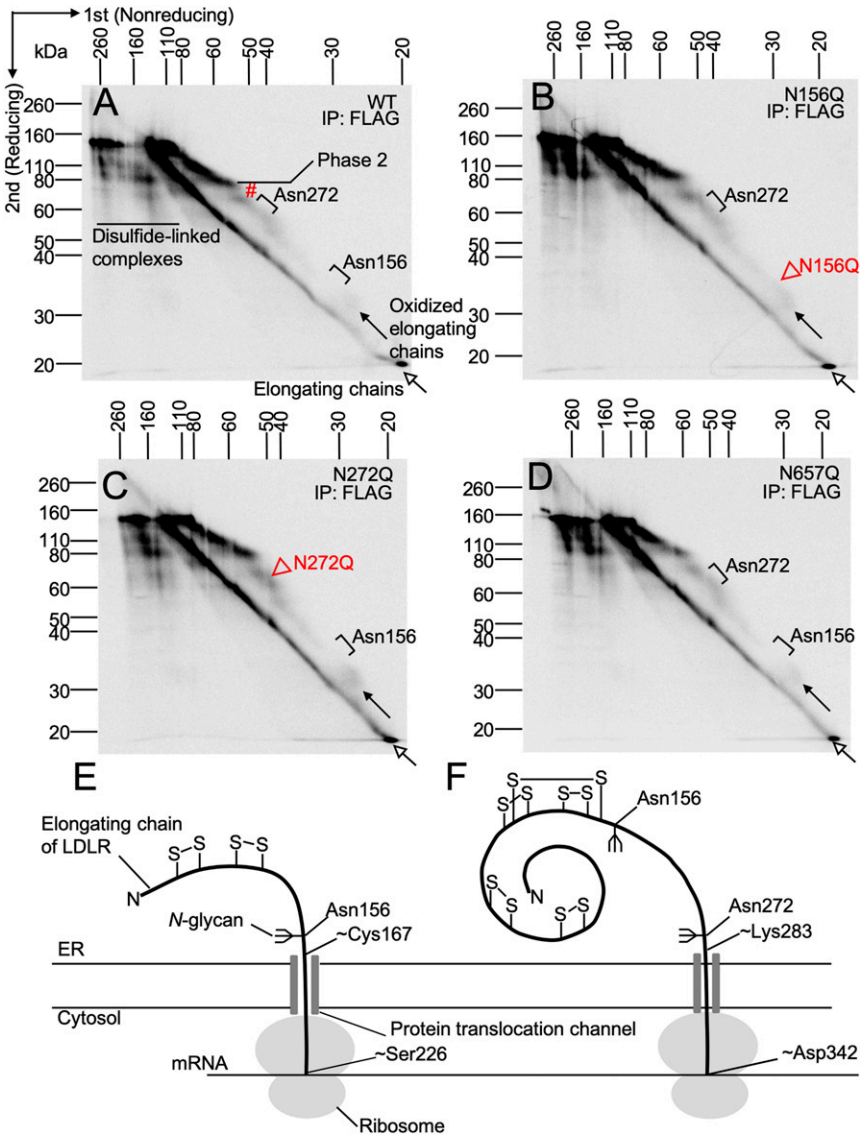

Fig. 2. Disulfide bond formation and N-glycosylation in LDLR analyzed by 2D SDS/PAGE. The elongating chains of LDLR, radiolabeled, and purified from HeLa cells expressing FLAG-LDLR (*A*), FLAG-LDLR N156Q (*B*), FLAG-LDLR N272Q (*C*), or FLAG-LDLR N657Q (*D*) were separated by 2D SDS/PAGE and detected by a phosphorimager. Open arrow, the elongating chains of LDLR; filled arrow, the oxidized elongating chains of LDLR. The regions of low radioactivity observed at ∼35 and ∼60 kDa on *A* (see brackets on the oxidized chains) disappeared upon mutating Asn156 and Asn272, respectively (see arrowheads in *B* and *C*). Thus, they correspond to *N*-glycan addition to Asn156 and Asn272, respectively. #, a region that is likely translated at a much higher rate than the surrounding codons. (*E* and *F*) Estimated topology of ribosome-bound LDLR chains at the timing of *N*-glycan addition to Asn156 (*E*) or Asn272 (*F*). Note that N-glycosylation requires that the residue that receives *N*-glycan is located at a minimal distance from the ER membrane of ∼11 amino acids (11). Accordingly, at the timings of N-glycosylation at Asn156 and Asn272, Cys167 and Lys283 are predicted to be near the luminal side of the ER membrane (*E* and *F*). Thus, the total numbers of cysteine residues exposed to the ER lumen would be 22 and 37, respectively, based on the amino acid sequence of LDLR. As described in *Results*, some disulfide bonds were already formed in the elongating chains at the timings of N-glycosylation at Asn156 and Asn272 (*E* and *F*). However, we do not have information on the precise numbers of disulfide bonds formed nor their exact connectivity.

form on the polypeptides before their elongation to Ser226 (Fig. 2*E*).

Whether Asn657 is glycosylated cotranslationally remains unclear, as we failed to observe any changes in gel pattern between the WT and N657Q mutant (Fig. 2 *A* and *D*). Furthermore, the region of low radioactivity reproducibly observed at ∼70 kDa (indicated by "#" in Figs. 2*A* and 3*A*) persisted even when any of the N-glycosylation sites on LDLR was eliminated (Fig. 2 *B*–*D*). Accordingly, the gap at ∼70 kDa may correspond to a sequence that is translated at a much higher rate than the surrounding codons. Notably, such a gap was commonly observed in LDLR variants (e.g., Fig. 3*C* and *SI Appendix*, Fig. S5 *A* and *C*; see Fig. 5 A and C) just before the onset of phase 2 (see below), including an LDLR variant lacking the third to sixth blades of the β-propeller (*SI Appendix*, Fig. S5*A*). However, since the gap was absent in an LDLR variant lacking the entire domain (see Fig. 5E), it may be caused by the N-terminal region of the β-propeller.

Cotranslational Folding of LDLR Is Highly Coordinated and Can Be Divided into Three Phases. We noticed that the cotranslational folding of LDLR can be divided into three phases depending on the steepness of the slopes of oxidized elongating chains observed on the 2D gel (Fig. 3*B*). On the gel, the greater mobility in the first dimension is caused by the compactness of the protein

generated by disulfide bond formation. Thus, the slope slightly steeper than the diagonal observed during phase 1 suggests that the growing polypeptides started to form some disulfides when they were elongated to 30 kDa and continued to form more disulfides during this phase. When the polypeptides were elongated to ~80 kDa, the steep slope was switched with a short gradual slope of phase 2 that was immediately followed by a moderate slope of phase 3. During phase 2, the electrophoretic mobility of the polypeptides was greatly reduced. The meaning of this event will be discussed in the next section. Interestingly, deleting the N-terminal three R domains caused shortening of phase 1 (Fig. 3*C*). Further deletion of all R domains caused disappearance of phases 1 and 2, leaving phase 3 (Fig. 3*D*). Thus, phases 1 and 2 appear to reflect the folding reactions of the R domains.

Use of a Conformational Antibody to Observe the Shuffling of Nonnative Disulfides to Native Ones in the R1 Domain. It is well-established that the shuffling of nonnative into native disulfide bonds during the "posttranslational" folding of LDLR is accompanied by a decrease in the electrophoretic mobility of the protein (19, 20, 27). This fact led to a model that the protein is first folded into a full-length compact structure that contains nonnative disulfides between distant cysteines. During folding, these long loops are substituted by smaller loops with native disulfides to yield more extended molecules, causing decreased electrophoretic mobility (19). The isomerization reaction had occurred over tens of minutes after synthesis and, thus, had been regarded as a rate-limiting step in the folding pathway (19, 20, 27).

Interestingly, we observed a similar decrease in the electrophoretic mobility of the oxidized elongating chains during phase 2 as described above (Figs. 2*A* and 3*B*). It suggests that disulfide bonds were shuffled at this "specific" timing of protein synthesis. To examine whether the reaction led to the formation of "native" disulfide bonds in LDLR, we used anti-LDLR C7 antibody that recognizes a conformational epitope in the R1 domain (Fig. 1*A*), provided that the native disulfide bonds are present, irrespective of denaturation by SDS (19, 20, 36). We have confirmed the properties of the antibody (*SI Appendix*, Figs. S2 and S3 and *Supplementary Results*). The same antibody had been used to follow posttranslational formation of native disulfide bonds in LDLR (19, 20). Remarkably, C7 precipitated the oxidized elongating chains only of phase 3 (Fig. 4*A*), suggesting that the R1 domain acquired correct disulfide bonds near the end of phase 2. Thus, nonnative disulfide bonds formed in the R domains during phase 1 were likely isomerized to native ones during phase 2.

Interpretation for the Presence of Both Oxidized and Reduced Elongating Chains of LDLR within Cells. Analysis of disulfide bond formation in the elongating chains of LDLR using 2D SDS/PAGE revealed that, while some of the elongating chains underwent cotranslational oxidative folding, the other failed to do so (their signals remained on the diagonal) (e.g., Figs. 2*A* and 3*A*), which tempts us to suspect that a portion of the elongating chains of LDLR failed to enter the ER cotranslationally, preventing their cotranslational oxidative folding. To examine if this could be the case, we looked at the N-glycosylation of newly synthesized LDLR as the majority of N-glycosylation sites on human glycoproteins are cotranslationally modified as they enter the ER lumen (11, 37).

To study the N-glycosylation of newly synthesized LDLR, we purified the elongating chains of LDLR, treated them with or

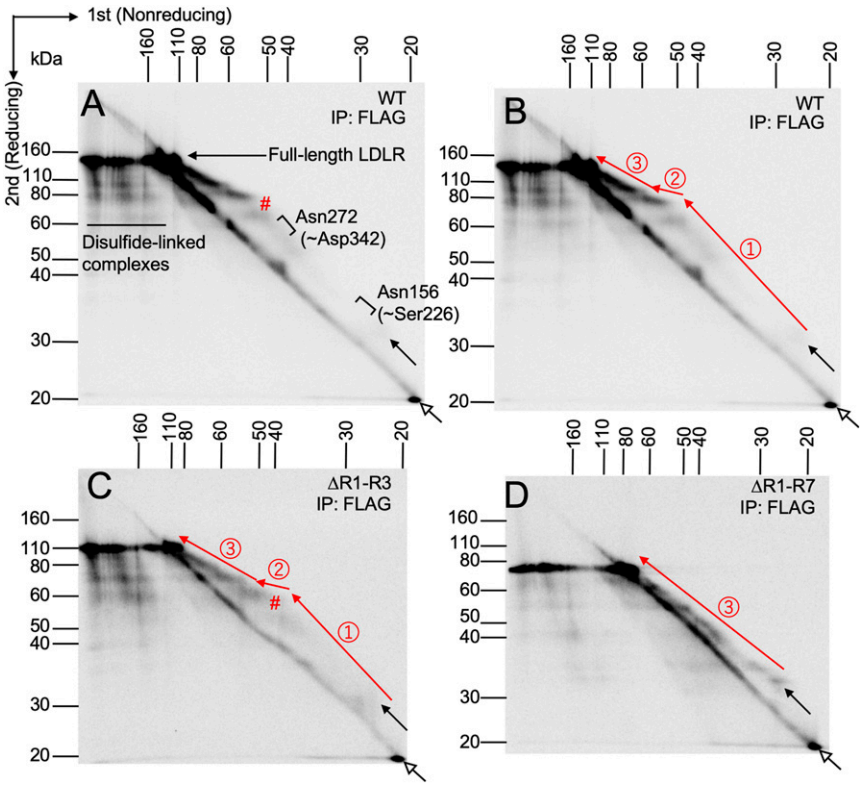

Fig. 3. Cotranslational folding of LDLR can be divided into three phases. The elongating chains of LDLR, radiolabeled and purified from cells expressing FLAG-LDLR (*A*), FLAG-LDLR ΔR1-R3 (*C*), or FLAG-LDLR ΔR1-R7 (*D*), were separated by 2D-SDS/PAGE. In *B*, the same gel as *A* was presented for explanation. Open arrow, the elongating chains of LDLR; filled arrow, the oxidized elongating chains of LDLR. (*A*) Brackets, the timings of *N*-glycan addition to Asp156 and Asn272; parentheses, the presumed C-terminal residue of the polypeptide at the timing of N-glycosylation. (*A* and *C*) #, a region that is likely translated at a much higher rate than the surrounding codons. (*B–D*) Red arrows, three phases of cotranslational folding.

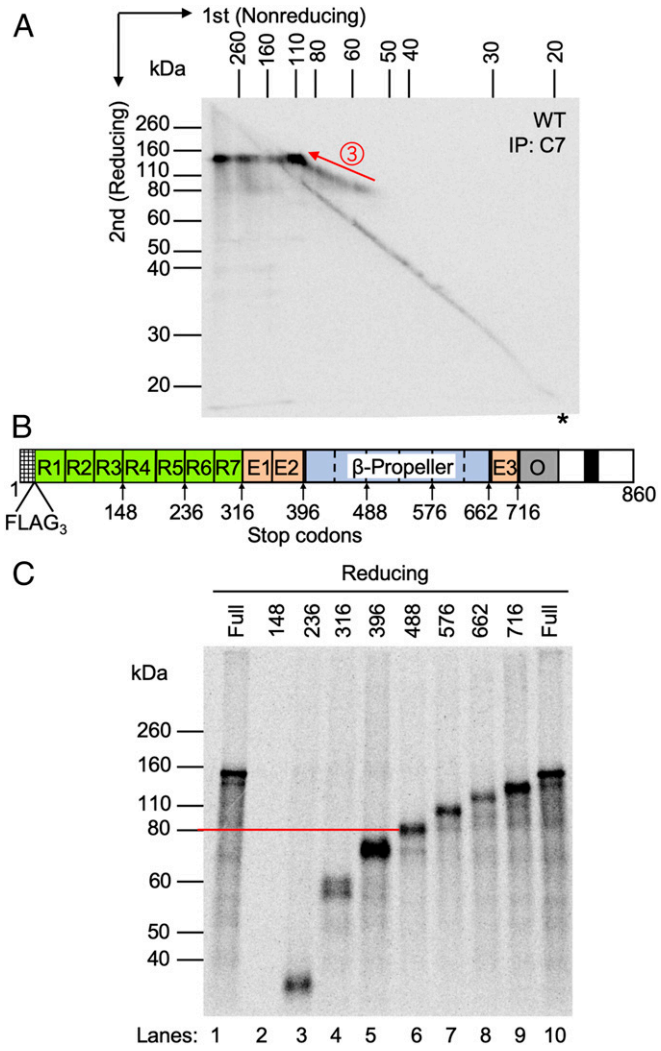

Fig. 4. Shuffling of nonnative disulfide bonds to native ones starts when the ribosome is translating the β-propeller region. (*A*) Cells expressing FLAG-LDLR were pulsed for 2 min, alkylated with NEM, immunoprecipitated with anti-LDLR C7 antibody (19), and separated by 2D SDS/PAGE. *, nonspecific signals (*SI Appendix*, Fig. S3). Note that anti-LDLR C7 antibody immunoprecipitated the oxidized elongating chains only of phase 3. (*B*) Positions of a stop codon in FLAG-LDLR truncation mutants. (*C*) The products from the indicated constructs, prepared as in Fig. 1*C*, were separated by reducing SDS/PAGE. Red line, the position of 80 kDa.

without endoglycosidase H (Endo H), and separated them by gel electrophoresis (*SI Appendix*, Fig. S4). On this gel, we observed two bands that correspond to the full-length LDLR. We propose for the following two reasons that the upper band represents the N-glycosylated full-length product of LDLR and the lower band the nonglycosylated full-length product of LDLR that failed to undergo oxidative folding. First, the digestion of *N*-glycan by Endo H converted the upper band to the lower band (*SI Appendix*, Fig. S4, lanes 1 and 3), indicating that the upper represents the N-glycosylated form of LDLR and the lower its nonglycosylated form. Second, when anti-LDLR C7 antibody was used to purify LDLR polypeptide that formed native disulfide bonds in the R1 domain, the upper band was efficiently recovered unlike the lower band, indicating that the upper represents LDLR that had undergone oxidative folding in the ER.

These observations indicate that there are two populations in the elongating chains of LDLR: those that underwent cotranslational translocation into the ER and oxidative folding in this compartment, and those that failed to undergo both N-glycosylation and oxidative folding cotranslationally. One possible explanation for the lack of these two modifications would be that the latter population failed to enter the ER cotranslationally. These findings and consideration can explain the coexistence of both oxidized and reduced elongating chains of LDLR within cells.

Phase 2 Starts while the Ribosome Is Translating the β-Propeller Domain. Phase 2 started when the polypeptide chains were elongated to ∼80 kDa (Fig. 3*B*). To estimate the position of the carboxyl end of the growing polypeptide at the beginning of phase 2, we constructed LDLR mutants each containing a stop codon at the C terminus of each domain or subdomain (Fig. 4*B*). A LDLR variant with a stop codon at the C terminus of the second subdomain (blade) of the β-propeller yielded a polypeptide chain of ∼80 kDa (Fig. 4*C*). Thus, phase 2 likely began when the ribosome was translating the middle of the β-propeller.

Shuffling of Nonnative Disulfides to Native Ones in the R1 Domain Requires the β-Propeller Region. Interestingly, deleting some of the R domains caused phase 2 to start at a shorter chain length (Figs. 3*C* and 5 *A* and *B*). It suggests the presence, in the downstream region, of a sequence that triggers the onset of phase 2, although some isolated R domains have been shown to fold properly but slowly in vitro (38).

To identify a region responsible for the cotranslational shuffling of disulfide bonds, we constructed LDLR variants lacking various domains. Deleting the EGF1 and EGF2 domains (Fig. 5 *C* and *D*) or the R domains other than R1 (Fig. 5 *A* and *B*) did not inhibit the cotranslational folding of R1, suggesting the nonessentiality of these domains in the cotranslational folding of R1. However, interestingly, deleting the β-propeller domain (Fig. 5 *E* and *F*) compromised the cotranslational folding of R1 as indicated by the disappearance of C7-positive signals on the oxidized elongating chains (Fig. 5*F*), demonstrating the importance of the β-propeller region in shuffling the nonnative disulfide bonds.

We further analyzed the cotranslational folding of LDLR lacking the C-terminal two or four blades of the β-propeller to verify that the entire domain was not essential for the shuffling but that the cotranslational folding of the upstream domains was improved progressively as the number of the blade was increased (*SI Appendix*, Fig. S5). These findings are consistent with the present observation that phase 2 started when the ribosome was translating the middle of the β-propeller (Fig. 4).

Discussion

Many mammalian cell-surface proteins including LDLR adopt multidomain structures and contain numerous disulfide bonds (13). Some of these proteins likely fold in the ER nonvectorially thorough intermediates with nonnative disulfide bonds (19–23). Shuffling of nonnative disulfide bonds, a key step in their folding, had been assumed to take place very slowly over tens of minutes after synthesis (13, 19–21), although it will take only ∼3 min to synthesize a protein like LDLR (760 amino acid long) given that the translation rate in mammalian cells is about three to five amino acids per second (13). Here, we found that the shuffling of nonnative disulfides in the R1 domain of LDLR takes place at a specific timing during synthesis, suggesting the presence of a sequence on LDLR that triggers the shuffling (Fig. 6). This assumption was validated by the discovery of a region on LDLR (the β-propeller) that was required for the reaction. The sharpness of the signals corresponding to phases 2 and 3 in WT LDLR (Figs. 2*A* and 3*A*) suggests that nonvectorial folding of a multidomain protein is a process much more coordinated and synchronized than thought when it occurs during synthesis (Fig. 6).

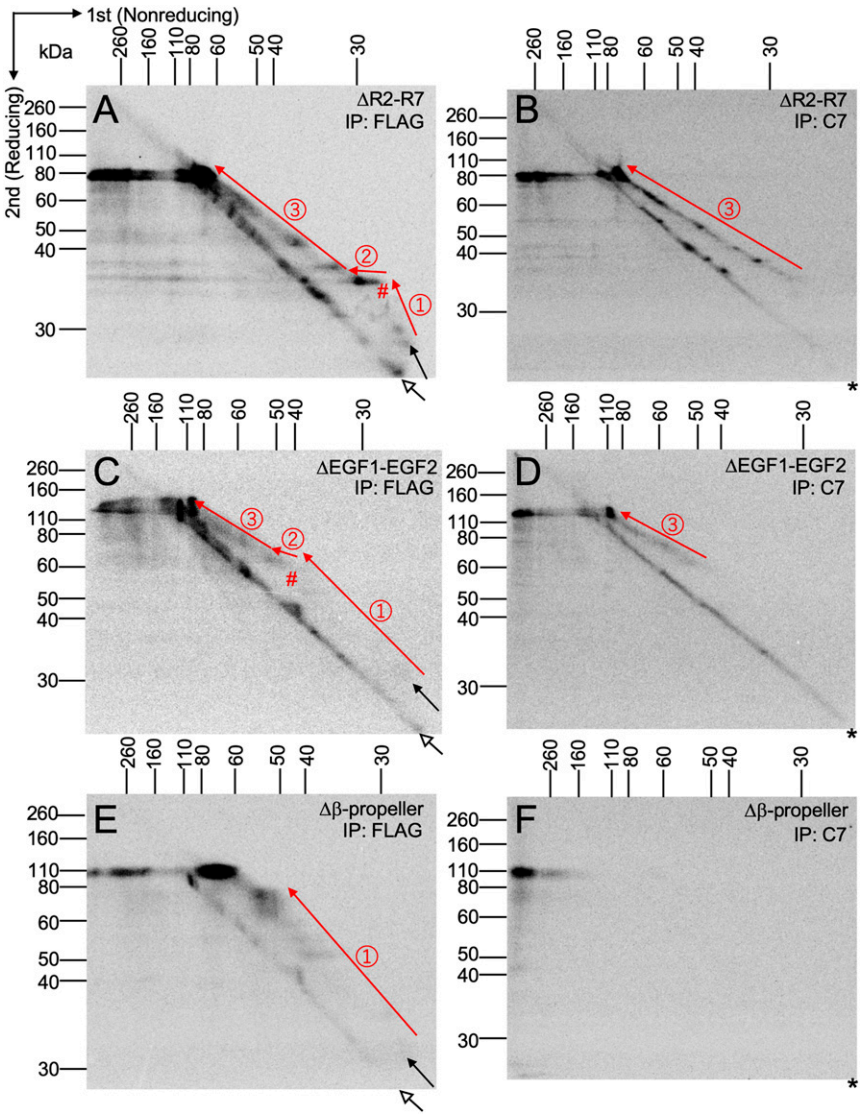

Fig. 5. The β-propeller region is required for the efficient cotranslational folding of LDLR. NEM-treated cell lysates, prepared as in Fig. 1*C* from cells expressing FLAG-LDLR ΔR2-R7 (*A* and *B*), FLAG-LDLR ΔEGF1-EGF2 (*C* and *D*), or LDLR Δβ-propeller (*E* and *F*), were immunoprecipitated with anti-FLAG (*A*, *C*, and *E*), or anti-LDLR C7 antibody (*B*, *D*, and *F*) and separated by 2D SDS/PAGE. Note that anti-LDLR C7 antibody immunoprecipitated the oxidized elongating chains only of phase 3 in *B* and *D*. Open arrow, the elongating chains of LDLR; closed arrow, the oxidized elongating chains of LDLR. Red arrows, three phases of cotranslational folding. #, a region that is likely translated at a much higher rate than the surrounding codons. *, nonspecific signals. Note also that nonspecific signals are less evident in *F* (see also *SI Appendix*, Fig. S3 legend).

In contrast to the previous model that the disulfide shuffling in the R1 domain of LDLR is a slow process requiring over tens of minutes after synthesis, we demonstrated here that it took place at a much earlier timepoint (that is during synthesis) when the oxidative folding had started cotranslationally. The merit of such "cotranslational" shuffling over "posttranslational" one will be that the domains can reach their native folded structures more quickly, decreasing the risk of their misfolding. Taking this advantage into account, we suggest that nonvectorial folding of some other multidomain proteins in the ER may also proceed cotranslationally.

Previous works that followed the behavior of newly synthesized full-length LDLR failed to observe that the shuffling of disulfide bonds in the R1 domain is a highly coordinated process that takes place at a specific timing during synthesis (19, 20). This fact underscores the importance of purifying and analyzing the growing polypeptide chains to discuss cotranslational oxidative folding process that takes place in cells, although the experiments are notoriously difficult and it is often required to expose the imaging plate to the gels of radiolabeled proteins for a long time (1 mo or more in our studies) to get signals (33).

It is still unclear why folding of some multidomain proteins in the ER proceeds via intermediates with nonnative disulfide bonds. One possibility is that some native disulfide bonds cannot be technically or efficiently introduced into a domain by PDI family members via a single oxidation reaction, necessitating prior formation of nonnative disulfide bonds and their subsequent shuffling to native ones (19, 39). In the case of LDLR, the latter reaction may be somehow assisted by a sequence in the β-propeller region.

Unlike template-assisted folding in which folding of a domain is facilitated by its assembly partner (13, 40–42), the β-propeller and its upstream domains are structurally independent of each other in the final fold (19, 25, 26). Thus, some multidomain

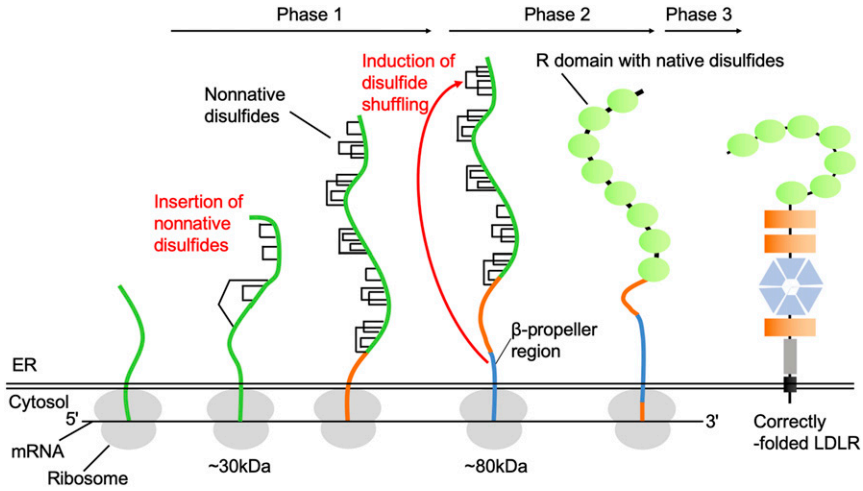

Fig. 6. Model for the cotranslational folding of LDLR. Note that the number and connectivity of nonnative disulfide bonds that form during phase 1 are unknown.

proteins may have evolved a sequence that can temporally assist in the folding of its structurally unrelated upstream domains.

Further analysis on the identity of the nonnative disulfide bonds that form during productive folding and the role of the downstream region in the shuffling reaction will help us define the principle for the nonvectorial folding of proteins in the ER of mammalian cells.

Materials and Methods

Plasmids. Plasmids used in this study are listed in *SI Appendix*, Table S1. Procedures for the construction of plasmids are described in *SI Appendix, Supplementary Materials and Methods*.

Cell Culture, Transfection, Pulse-Chase, and Alkylation. HeLa cells were maintained in Dulbecco's modified Eagle's medium (DMEM) (catalog no. 08458; Nacalai Tesque) supplemented with 10% fetal bovine serum (FBS) at 37 °C in 5% CO_2 air.

For transfection, HeLa cells were often plated onto a 6-cm dishes at 5×10^5 cells per dish, cultured for 24 h, and transfected with 3 μg of DNA using Lipofectamine LTX (Invitrogen), following manufacturer's instruction. At 24 h after transfection, cells were incubated in 1.5 mL per dish of depletion medium (Gibco Met-free, Cys-free DMEM supplemented with 2 mM L-glutamine, 1 mM sodium pyruvate, and 5% dialyzed FBS) for 30 min and pulse-labeled with 55 μCi/mL of EasyTag EXPRESS35S Protein Labeling Mix (PerkinElmer) for 2 min. When chase was conducted, cells were washed with phosphate-buffered saline (PBS) and then incubated in 1.5 mL of chase medium (DMEM supplemented with 10% FBS, 5 mM L-methionine, and 5 mM L-cysteine) to initiate the chase period. Following pulse or chase, cells were washed twice with PBS, directly treated with 1 mL of ice-cold 10% trichloroacetic acid, and collected in a tube. After 20-min incubation on ice, proteins were collected by centrifugation and washed twice with ice-cold acetone to remove acid. Free cysteines in the sample were then alkylated with NEM using NEM alkylation buffer (100 mM Tris·HCl [pH 6.8], 2% SDS, 50 mM NEM) supplemented with 2 μg/mL pepstatin A, 1 mM benzamidine, and 1 mM phenylmethylsufony fluoride (PMSF) essentially as described before (43).

Antibodies. Mouse anti-FLAG M2 and anti-LDLR C7 antibodies were purchased from Sigma-Aldrich and Santa Cruz Biotechnology, respectively. Rabbit monoclonal anti-LDLR EP1553Y antibody that recognizes the C terminus of LDLR was obtained from Abcam.

Immunoprecipitation. To purify LDLR polypeptides fused with a triple FLAG tag, 150 μg of NEM-treated HeLa cell lysate (see above) was diluted 10-fold with ice-cold KI buffer (2% [wt/vol] Triton X-100, 50 mM Tris·HCl [pH 8.0], 150 mM NaCl, 1 mM EDTA) and centrifuged at 15,000 × *g* for 10 min at 4 °C to obtain NEM-treated cleared cell lysate. To purify LDLR polypeptides containing the triple FLAG tag from the cleared cell lysate, mouse anti-FLAG M2 antibody was bound to Surebeads protein G magnetic beads (Bio-Rad) in the presence of ice-cold KI buffer following the supplier's instructions. The resulting beads were incubated with the NEM-treated cleared cell lysate for 3 h at 4 °C. The immune complexes were collected by magnetization and washed four times with 800 μL of ice-cold High Salt buffer (1% [wt/vol] Triton X-100, 50 mM Tris·HCl [pH 8.0], 1 M NaCl, 1 mM EDTA), and once with 800 μL of 10 mM Tris·HCl (pH 8.0). The immunoisolates were then released by incubating the sample at 37 °C for 1 h with 65 μL of 2× Laemmli sample buffer supplemented with 10 mM NEM, 2 μg/mL pepstatin A, 1 mM benzamidine, and 1 mM PMSF.

To purify LDLR polypeptides that have acquired correct disulfide bonds in the R1 domain, 300 μg of NEM-treated HeLa cell lysate (see above) was diluted 10-fold with ice-cold KI buffer containing 2 mM $CaCl_2$ and then centrifuged at 15,000 × *g* for 10 min at 4 °C to obtain NEM-treated cleared cell lysate. LDLR polypeptides that have acquired correct disulfide bonds in the R1 domain were then purified from the cleared lysate using anti-LDLR C7 antibody bound to Surebeads protein A magnetic beads (Bio-Rad) essentially as described above except that the immune complexes were washed six times with ice-cold High Salt buffer and once with 10 mM Tris·HCl (pH 8.0) before releasing the immunoisolates.

Nonreducing, Reducing 2D Gel Electrophoresis. Ten microliters of immunoprecipites from the pulsed samples were separated on a nonreducing 10% SDS/PAGE. The gel lanes were cut off, incubated in gel reducing buffer (75 mM Tris·HCl [pH 6.8], 2% [wt/vo] SDS, 15% [wt/vol] glycerol, 5% [vol/vol] β-mercaptoethanol, and 10 μg/mL bromophenol blue) at 80 °C for 10 min. The proteins in the gel were then separated on a 2D gel, dried on a filter paper, and detected by an imaging plate, BAS IP MS 2040 E (GE Healthcare) and a PhosphorImager FLA-2000 (Fuji Film). To observe changes in the oxidation states of the elongating chains of LDLR on the 2D gel, we exposed the imaging plate to the dried gels from 1 to 3 mo. We added 5 μL of Novex Sharp Prestained Protein Standard (Thermo Fisher Scientific) to the immunoprecipitates just before running the 1D gel to confirm the proper protein separation on a 2D gel. If separated properly, the marker proteins will migrate on a diagonal as sharp spots on the 2D gel. Otherwise, we repeated the gel electrophoresis. We used Novex Sharp Prestained Protein Standard (Thermo Fisher Scientific), as maker proteins for gel electrophoresis as reductant is not added to its loading buffer and, thus, this reagent does not perturb the migration of oxidized proteins in adjacent lanes.

Data Availability. All data and associated protocols are available in the main text and *SI Appendix*.

ACKNOWLEDGMENTS. We are grateful to Hisayuki Mitsui and Kouki Konno in the Radioisotope Facility of Graduate School of Life Sciences, Tohoku University, supporting the experiments involving radioisotope. We also thank Koreaki Ito, Hideki Taguchi, Kenji Kohno, and Shinobu Chiba for helpful discussions. This work was supported by Japan Society for the Promotion of Science (JSPS) Grants-in-Aid for Scientific Research (KAKENHI) Grant JP19H02881 (to H.K.) and the Ministry of Education, Culture, Sports, Science, and Technology (MEXT) KAKENHI Grant JP26116005 (to H.K. and K.I.).

1. J. H. Han, S. Batey, A. A. Nickson, S. A. Teichmann, J. Clarke, The folding and evolution of multidomain proteins. *Nat. Rev. Mol. Cell Biol.* **8**, 319–330 (2007).
2. K. C. Stein, J. Frydman, The stop-and-go traffic regulating protein biogenesis: How translation kinetics controls proteostasis. *J. Biol. Chem.* **294**, 2076–2084 (2019).
3. T. Tanaka, N. Hori, S. Takada, How co-translational folding of multi-domain protein is affected by elongation schedule: Molecular simulations. *PLOS Comput. Biol.* **11**, e1004356 (2015).
4. H. K. Choi *et al*., Watching helical membrane proteins fold reveals a common N-to-C-terminal folding pathway. *Science* **366**, 1150–1156 (2019).
5. W. M. Jacobs, E. I. Shakhnovich, Evidence of evolutionary selection for cotranslational folding. *Proc. Natl. Acad. Sci. U.S.A.* **114**, 11434–11439 (2017).
6. K. Liu, X. Chen, C. M. Kaiser, Energetic dependencies dictate folding mechanism in a complex protein. *Proc. Natl. Acad. Sci. U.S.A.* **116**, 25641–25648 (2019).
7. M. B. Borgia *et al*., Single-molecule fluorescence reveals sequence-specific misfolding in multidomain proteins. *Nature* **474**, 662–665 (2011).
8. A. Lafita, P. Tian, R. B. Best, A. Bateman, Tandem domain swapping: Determinants of multidomain protein misfolding. *Curr. Opin. Struct. Biol.* **58**, 97–104 (2019).
9. K. C. Stein, A. Kriel, J. Frydman, Nascent polypeptide domain topology and elongation rate direct the cotranslational hierarchy of Hsp70 and TRiC/CCT. *Mol. Cell* **75**, 1117–1130.e5 (2019).
10. C. F. Wright, S. A. Teichmann, J. Clarke, C. M. Dobson, The importance of sequence diversity in the aggregation and evolution of proteins. *Nature* **438**, 878–881 (2005).
11. R. Daniels, B. Kurowski, A. E. Johnson, D. N. Hebert, N-linked glycans direct the cotranslational folding pathway of influenza hemagglutinin. *Mol. Cell* **11**, 79–90 (2003).
12. M. Okumura, H. Kadokura, K. Inaba, Structures and functions of protein disulfide isomerase family members involved in proteostasis in the endoplasmic reticulum. *Free Radic. Biol. Med.* **83**, 314–322 (2015).
13. L. Ellgaard, N. McCaul, A. Chatsisvili, I. Braakman, Co- and post-translational protein folding in the ER. *Traffic* **17**, 615–638 (2016).
14. M. J. Feige, I. Braakman, L. Hendershot, "Disulfide bonds in protein folding and stability" in *Oxidative Folding of Proteins: Basic Principles, Cellular Regulation and Engineering*, M. J. Feige, Ed. (Royal Society of Chemistry, 2018), pp. 1–33.
15. T. Anelli, R. Sitia, "Mechanisms of oxidative protein folding and thiol-dependent quality control: Tales of cysteines and cystines" in *Oxidative Folding of Proteins: Basic Principles, Cellular Regulation and Engineering*, M. J. Feige, Ed. (Royal Society of Chemistry, 2018), pp. 249–266.
16. I. Braakman, N. J. Bulleid, Protein folding and modification in the mammalian endoplasmic reticulum. *Annu. Rev. Biochem.* **80**, 71–99 (2011).
17. L. W. Bergman, W. M. Kuehl, Formation of an intrachain disulfide bond on nascent immunoglobulin light chains. *J. Biol. Chem.* **254**, 8869–8876 (1979).
18. W. Chen, J. Helenius, I. Braakman, A. Helenius, Cotranslational folding and calnexin binding during glycoprotein synthesis. *Proc. Natl. Acad. Sci. U.S.A.* **92**, 6229–6233 (1995).
19. A. Jansens, E. van Duijn, I. Braakman, Coordinated nonvectorial folding in a newly synthesized multidomain protein. *Science* **298**, 2401–2403 (2002).
20. F. Pena, A. Jansens, G. van Zadelhoff, I. Braakman, Calcium as a crucial cofactor for low density lipoprotein receptor folding in the endoplasmic reticulum. *J. Biol. Chem.* **285**, 8656–8664 (2010).
21. A. Land, D. Zonneveld, I. Braakman, Folding of HIV-1 envelope glycoprotein involves extensive isomerization of disulfide bonds and conformation-dependent leader peptide cleavage. *FASEB J.* **17**, 1058–1067 (2003).
22. G. J. Poet *et al*., Cytosolic thioredoxin reductase 1 is required for correct disulfide formation in the ER. *EMBO J.* **36**, 693–702 (2017).
23. B. S. Roberts, M. A. Babilonia-Rosa, L. J. Broadwell, M. J. Wu, S. B. Neher, Lipase maturation factor 1 affects redox homeostasis in the endoplasmic reticulum. *EMBO J.* **37**, 1–17 (2018).
24. T. C. Südhof, J. L. Goldstein, M. S. Brown, D. W. Russell, The LDL receptor gene: A mosaic of exons shared with different proteins. *Science* **228**, 815–822 (1985).
25. J. Gent, I. Braakman, Low-density lipoprotein receptor structure and folding. *Cell. Mol. Life Sci.* **61**, 2461–2470 (2004).
26. H. Jeon, S. C. Blacklow, Structure and physiologic function of the low-density lipoprotein receptor. *Annu. Rev. Biochem.* **74**, 535–562 (2005).
27. O. B. V. Oka, M. A. Pringle, I. M. Schopp, I. Braakman, N. J. Bulleid, ERdj5 is the ER reductase that catalyzes the removal of non-native disulfides and correct folding of the LDL receptor. *Mol. Cell* **50**, 793–804 (2013).
28. M. Koritzinsky *et al*., Two phases of disulfide bond formation have differing requirements for oxygen. *J. Cell Biol.* **203**, 615–627 (2013).
29. H. Kadokura, J. Beckwith, Detecting folding intermediates of a protein as it passes through the bacterial translocation channel. *Cell* **138**, 1164–1173 (2009).
30. K. Yanagitani, Y. Kimata, H. Kadokura, K. Kohno, Translational pausing ensures membrane targeting and cytoplasmic splicing of XBP1u mRNA. *Science* **331**, 586–589 (2011).
31. T. Fujimoto, K. Inaba, H. Kadokura, Methods to identify the substrates of thiol-disulfide oxidoreductases. *Protein Sci.* **28**, 30–40 (2019).
32. M. Molinari, A. Helenius, Glycoproteins form mixed disulphides with oxidoreductases during folding in living cells. *Nature* **402**, 90–93 (1999).
33. M. Molinari, A. Helenius, Analyzing cotranslational protein folding and disulfide formation by diagonal sodium dodecyl sulfate-polyacrylamide gel electrophoresis. *Methods Enzymol.* **348**, 35–42 (2002).
34. N. B. Pedersen *et al*., Low density lipoprotein receptor class A repeats are O-glycosylated in linker regions. *J. Biol. Chem.* **289**, 17312–17324 (2014).
35. K. Braunger *et al*., Structural basis for coupling protein transport and N-glycosylation at the mammalian endoplasmic reticulum. *Science* **360**, 215–219 (2018).
36. A. T. Nguyen, T. Hirama, V. Chauhan, R. Mackenzie, R. Milne, Binding characteristics of a panel of monoclonal antibodies against the ligand binding domain of the human LDLr. *J. Lipid Res.* **47**, 1399–1405 (2006).
37. N. Cherepanova, S. Shrimal, R. Gilmore, N-linked glycosylation and homeostasis of the endoplasmic reticulum. *Curr. Opin. Cell Biol.* **41**, 57–65 (2016).
38. O. Szekely *et al*., Identification and rationalization of kinetic folding intermediates for a low-density lipoprotein receptor ligand-binding module. *Biochemistry* **57**, 4776–4787 (2018).
39. Y. Sato *et al*., Synergistic cooperation of PDI family members in peroxiredoxin 4-driven oxidative protein folding. *Sci. Rep.* **3**, 2456 (2013).
40. L. W. Bergman, W. M. Kuehl, Formation of intermolecular disulfide bonds on nascent immunoglobulin polypeptides. *J. Biol. Chem.* **254**, 5690–5694 (1979).
41. S.-S. Chng *et al*., Disulfide rearrangement triggered by translocon assembly controls lipopolysaccharide export. *Science* **337**, 1665–1668 (2012).
42. M. J. Feige, J. Behnke, T. Mittag, L. M. Hendershot, Dimerization-dependent folding underlies assembly control of the clonotypic $\alpha\beta$T cell receptor chains. *J. Biol. Chem.* **290**, 26821–26831 (2015).
43. T. Fujimoto *et al*., Identification of the physiological substrates of PDIp, a pancreas-specific protein-disulfide isomerase family member. *J. Biol. Chem.* **293**, 18421–18433 (2018).